Comparison of Strategies for Landmine Modeling in LS-DYNA with Sandy Soil Material Model Development

Matt Barsotti; Eric Sammarco, Ph.D., P.E.; David Stevens, Ph.D., P.E.
Protection Engineering Consultants (PEC)

Abstract

As part of the United States Marine Corps (USMC) Mitigation of Blast Injuries through Modeling and Simulation project, Protection Engineering Consultants investigated and compared a range of landmine modeling strategies in LS-DYNA. Dividing the constituent materials into solids (soil) and fluids (air and explosive burn products), various numerical formulations were applied to the two groups in different combinations. Single-formulation strategies included a traditional all-ALE approach and a less conventional all-SPH approach. Hybrid formulation strategies included combinations of ALE fluid and explosive materials with FEM, DEM, or SPH soil. The various single-formulation and hybrid-formulation are compared in terms of implementation, required coupling definitions, stability issues, calculation demands, and overall feasibility.

The quantitative performance of three front-runner strategies were compared against benchmark test data. Evaluation cases included initial soil bubble formation, scaled-test impulses against flat plates, scaled-test impulses against angled plates, and full-scale impulses against flat plates. The benchmark tests used sandy soils at varying levels of saturation.

A generalized sandy soil modeling approach was used to generate parameters for the Pseudo Tensor material model and the Tabulated Compaction equation of state. The average error for predicted impulse was less than 2.5%, which was obtained from the generalized soil model using a priori material parameter settings and without post hoc tuning.

Modeling Strategies

A number of different numerical modeling strategies for simulating landmine detonations were considered. ALE and SPH formulations were both used to model the complete mine problem, including soil, air, and explosive. Three hybrid approaches were also considered, which separated the air/explosive from the soil, using ALE for the former and FEM, SPH, or DEM for the latter.

		Soil Formulation			
		ALE	FEM	SPH	DEM
HE & Air Formulation	ALE	✓	✓	✓	✓
	FEM				
	SPH			✓	
	DEM				

The full Arbitrary Lagrangian Eulerian (ALE) approach was taken as the historical baseline for the effort. The two primary shortfalls of the ALE formulation include the need for a large domain that engulfs the target vehicle undercarriage and the need for fluid-structure interaction (FSI) coupling algorithms (*CONSTRAINED_LAGRANGE_IN_SOLID). The former produces a computational burden on the simulation, while the latter can be plagued by leakage and stability issues.

The full Smoothed Particle Hydrodynamics (SPH) approach avoids the ALE domain size requirements, since separate particles can transit unlimited distances without an intervening fluid

containment mesh. It also eliminates complications arising from FSI, since normal Lagrangian contacts may be used for mine-vehicle interactions. Drawbacks include a higher 1:1 computational expense than ALE, in part because the code must repeatedly parse the model domain to determine which particles are in proximity to one another. The comparative cost is further exacerbated because SPH typically requires a finer discretization to obtain similar accuracy; it is not uncommon to employ an 8:1 ratio in 3D models. Finally, the drastic difference in density between air and soil requires the use of particle-to-particle contact at the air-soil interface (*DEFINE_SPH_TO_SPH_COUPLING), which can be the source of significant intrinsic instability.

The hybrid ALE-SPH approach represented soil near the explosive charge with SPH particles, while the explosive and air constituents were modeled using ALE. This hybrid helped to mitigate SPH computational expense, and it was considered the most organic representation of the granular nature of the soil material and the fluid nature of air and explosive products. Soil far from the charge was represented with finite element bricks. The ALE explosive loaded the SPH soil particles through FSI penalty coupling (*ALE_COUPLING_NODAL_PENALTY).

The hybrid ALE-FEM approach was inspired by literature that featured the modeling of soil with eroding finite elements (1) (2). Within LS-DYNA, the eroding elements can be either converted into deleted nodes or into SPH particles. The deleted node approach can lead to a fictitious loss of soil volume which reduces the confinement on the expanding gas products. Converting deleted elements to SPH particles offered a more elegant solution that was capable of retaining soil volume while still adapting to extreme deformations (*DEFINE_ADAPTIVE_SOLID_ TO_SPH). This LS-DYNA option was nominally comparable to the manner in which EPIC converts distorted finite elements into GPA particles (2). In practice, however, the LS-DYNA conversion proved numerically unstable. The explosive and air were modeled with ALE materials, and the FSI coupling during erosion seemed numerically fragile. As the code attempted to transition the explosive coupling from the soil finite elements to the newly-formed soil SPH particles, error terminations often resulted (i.e., from *CONSTRAINED_LAGRANGE _IN_SOLID to *ALE_COUPLING_NODAL_PENALTY). At present, this capability within LS-DYNA seems to lack the necessary maturity for reliable use. This paper omits further discussion of this approach.

The hybrid ALE-DEM approach was considered since the discrete element method (DEM) has risen in popularity over the last several years. Some codes, such as IMPETUS, model landmines exclusively with DEM (3). Yet DEM differs notably from ALE, FEM, and SPH, all of which rely on continuum mechanics to define materials with a combination of strength model and compaction model. DEM consists instead of a collection of rigid mass particles that interact via spring-damper contact definitions. Tuning a DEM definition to accurately represent landmine behavior requires a series of landmine tests conducted on that specific soil. Practically speaking, however, there is no intrinsic bridge from material properties (derived from laboratory tests) to landmine predictions. We note that LSTC appears to be developing a generalized material mapping capability that could populate DEM coefficients directly from standard constitutive models (*DEFINE_DE_HBOND). However, that capability was not fully functional during the project, and it was not clear whether it would extend to the complexities of pressure-dependent soil properties or be functional across the demanding load range present within landmine models. After initial trials and material property considerations, pursuit of DEM was suspended, and this paper omits further related discussion.

Sandy Soil Material Model Development

Development of a robust and accurate approach for soil modeling was a significant accomplishment of the effort. Regardless of the modeling strategy used (FEM, ALE, SPH, etc.), the accuracy of landmine blast loads appears to be strongly driven by the fidelity of the soil material model. Since many benchmark landmine tests have been performed on sandy soils of varying moisture contents, ranging from dry to fully saturated, soil modeling efforts were focused on sand.

A detailed literature survey was conducted, including some ninety technical papers and reports, in which major paradigmatic approaches, research families, and institutions were recognized and catalogued. Although a detailed review is beyond the scope of this paper, key research that informed our efforts included noted references from the US Army Engineer Research and Development Center (ERDC), Army Research Laboratory (ARL), US Army Tank-Automotive Research Development and Engineering Center (TARDEC), Aberdeen Proving Ground (APG), Defense Nuclear Agency, Canadian Defence Research Establishment Suffield (DRES), Norwegian Geotechnical Institute (NGI), Southwest Research Institute (SwRI), Ernst Mach Institute (EMI), Clemson University (CU), Sandia National Laboratories (SNL), Schwer Engineering and Consulting Services, and the Wright Laboratory Flight Dynamics Directorate. See references: (1) (2) (4) (5) (6) (7) (8) (9) (10) (11) (12) (13) (14) (15) (16) (17) (18). A full literature review and description of the technical effort may be found in the USMC SBIR report (19).

Protection Engineering Consultants (PEC) decided to develop an independent approach to modeling sandy soil that would be accurate in predicting landmine loads using *a priori* definitions determined by normal soil constitutive properties, without requiring recourse to *post hoc* material tuning. Conceptually, our approach is perhaps most similar to the Kerley method described by Anderson (6); however, our alignment with Kerley on various specific points remains uncertain. As will be shown in the subsequent sections, our material modeling approach within LS-DYNA has yielded accurate predictions, with error measures being reduced by an order of magnitude compared with some of the approaches noted in the literature.

Baseline Sand Properties

The baseline material properties used to represent sandy soils were derived from two primary sources. The majority of the properties are based upon Sjobo sand, as characterized by Laine & Sandvik (11), which included compaction, strength, and modulus (11). Yield strength properties for varying levels of saturation were derived from Kerley (9) (12). For dry sand, Laine and Kerley show nominal agreement.

Dry Density Modifications

Modification of the Sjobo properties to represent alternate dry densities was considered relatively straightforward. It was assumed that the terminal density and modulus of fully compacted sand was nominally the same for different species, i.e., that of pure quartz (ρ = 2,650 kg/m^3). Variations in dry density can be influenced by particulate gradation, particulate sphericity, and material consolidation arising from tamping or vibration. The ratio of the loose and terminal density for Sjobo sand indicates a void fraction of approximately 37%. For higher or lower dry

sand densities, the pressure-density curve was either compressed or dilated from the left end while leaving the terminal density unaltered.

Saturation Modifications

Two major modifications were made to the soil to account for an arbitrary level of saturation. First, the yield strength was modified per Kerley (12). The initial slope of the yield surface remained that of dry Sjobo sand, but the flat-line strength plateau was adjusted.

The second modification involved altering the compaction curve, which was a more complex undertaking. The sand compaction curve was separated into two components. The first was a semi-parabolic load curve representing pressure versus volumetric strain for the void space compaction of the dry soil skeleton, up to the terminal lockup point. The second part represented the terminal lockup in which no voids remain in the sand, which was effectively the bulk modulus of quartz. A third component for water was defined by the Gruneisen equation of state, which defines a semi-parabolic curve that has a vertical asymptote at a volumetric strain of ~0.5. These three components were merged into a three-spring model, depicted by the simplified one-dimensional schematic of Figure 1. Two of the spring elements (K_W & K_V) were nonlinear, and the gauge length of each element was determined based upon the void fraction and saturation level of the soil. Using the three-spring relationship, the compaction curve for any sand is defined by calculating the net spring resistance across the full range of compression strains. It should be noted that for the case of fully saturated sand, the initial modulus produced by this spring system matches that given by the Wood equation (13).

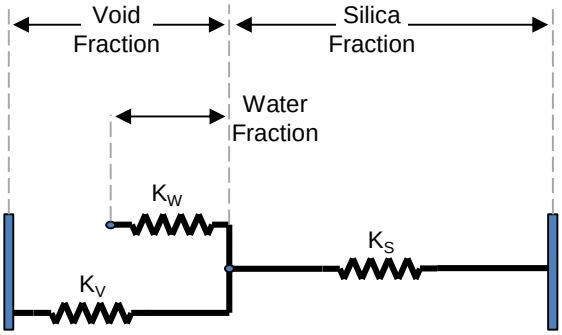

Figure 1. Element Schematic of Three-Spring Compaction Model

The bounding behavior of the three-spring model was verified by calculating the net compression resistance for pure Sjobo sand and pure water, both of which overlay their respective reference curves correctly. When applied to varying saturation levels, the three-spring model produced compression curves that demonstrated the expected water lockup behavior, plotted for clarity in engineering strain (Figure 2). The compaction curves were defined throughout the full volumetric strain regime, as is required for landmine models in which the material in immediate contact with the charge is compressed to the terminal quartz limit.

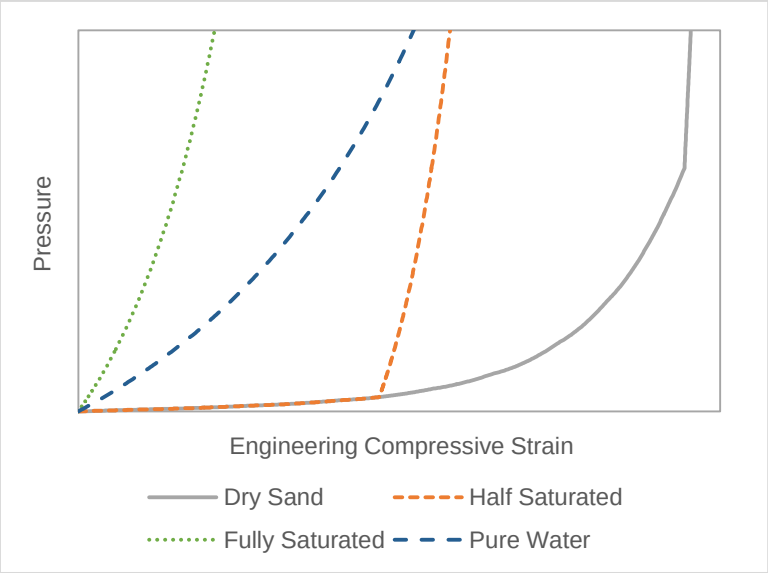

Figure 2. Typical Compaction Curves for Sand at Varying Levels of Saturation

LS-DYNA Keywords

In LS-DYNA, the soil was modeled using two keywords. The elastic properties and yield strength were modeled with *MAT_PSEUDO_TENSOR (*MAT_016, Mode I). The strength versus pressure yield surface was defined as a simple bilinear curve with a maximum strength plateau per Kerley. The compaction behavior and unloading modulus were defined using the equation of state *EOS_TABULATED_ COMPACTION, which was populated per the three spring methodology described above.

The explosive materials C-4 and Comp-B were represented in LS-DYNA with the *MAT_HIGH_EXPLOSIVE_BURN material model and the *EOS_JWL equation of state. Their parameters were populated using the CTH material database. Air was modeled at gauge pressure in LS-DYNA using the *MAT_NULL material model and the *EOS_LINEAR_POLYNOMIAL equation of state.

Models of Soil Expansion

The Defence Research Establishment Suffield (DRES) in Alberta Canada carried out an experimental test program aimed at studying the basic explosion physics of shallow-buried charges (10) (17). The test series involved the detonation of C-4 explosive disks weighing nominally 100-g when buried at various depths within a barrel of sand.

LS-DYNA was used to simulate these soil expansion tests with the ALE, SPH, and hybrid ALE-SPH strategies for 3-cm and 8-cm depth of burial (DOB) cases, using a 3-dimensional, quarter-symmetry computational domain. The typical ALE element size was 3-mm (10 elements or more through thickness of soil cap), and the computational domain was nominally 295-mm by 295-mm in plan and 594-mm in elevation (318-mm of air plus 276-mm of soil). Figure 3 shows experimental and model soil bubble profiles for the 8-cm DOB (left) and a comparison of expansion trends for both DOB.

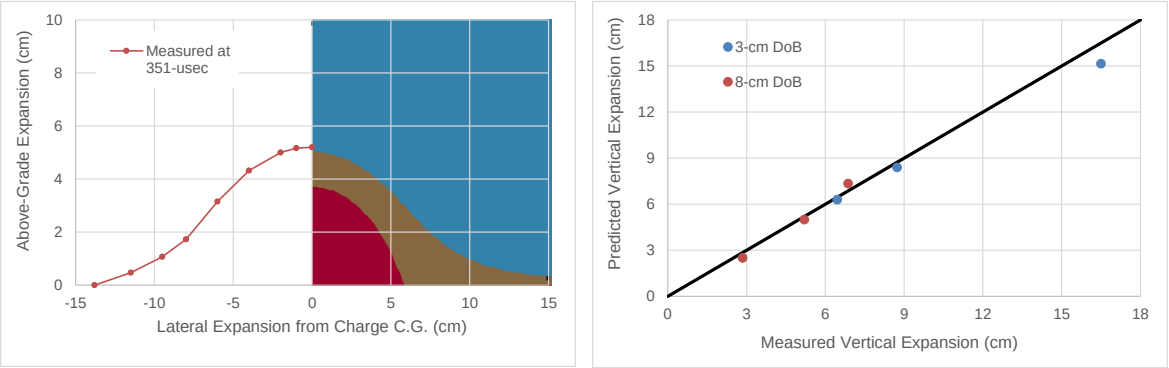

Figure 3. 8-cm DOB Soil Expansion Simulation for ALE Modeling Strategy, PEC Soil Model; Measurements Adapted from (17)

The pure SPH simulations were carried out with a 3-dimensional, quarter-symmetry computational domain. Typical particle spacing was 1.5-mm, or one-half that of the comparable ALE model, and the quarter-symmetry computational domain size was nominally 150-mm by 150-mm in plan and 276-mm of soil in elevation. Due to identified numerical instabilities involving SPH air particles, air was neglected during these simulations. Figure 4 shows experimental and model soil bubble profiles for the 8-cm DOB (left) and a comparison of expansion trends for both DOB. In comparing the ALE trend of Figure 3 and the SPH trend of Figure 4, it is clear that the SPH modeling strategy is less accurate and seems to enhance the ALE error trends, alternately yielding under- and over-predicted expansions.

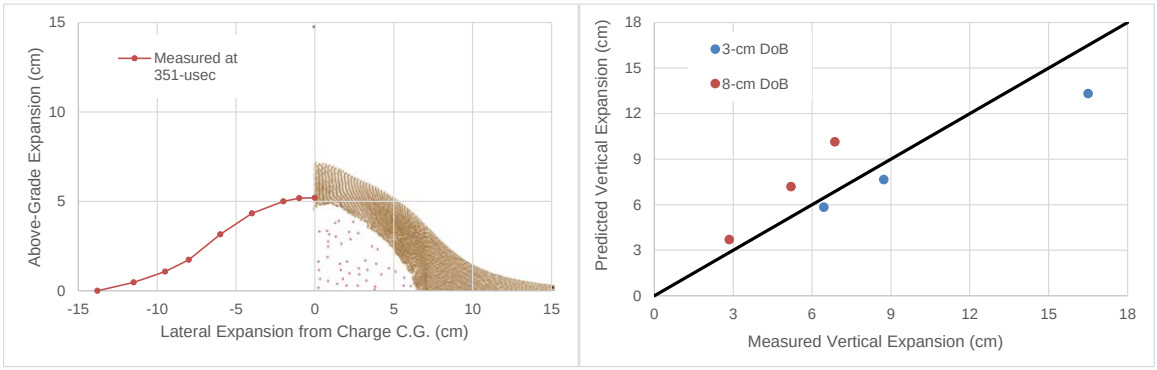

Figure 4. 8-cm DOB Soil Expansion Simulation for SPH Modeling Strategy; Measurements Adapted from (17)

The hybrid ALE-SPH simulations were carried out with a 3-dimensional, quarter-symmetry computational domain. Typical SPH particle spacing was 1.5-mm, and the typical ALE element size was 3-mm (i.e., an 8-to-1 SPH-to-ALE ratio was employed, where 8 SPH particles could fit into a single ALE element volume). The quarter-symmetry computational domain size was nominally 150-mm by 150-mm in plan and 416-mm in elevation (216-mm of ALE air plus 200-mm of SPH soil). Figure 5 shows experimental and model soil bubble profiles for the 8-cm DOB (left) and a comparison of expansion trends for both DOB. The results show that the hybrid ALE-SPH formulation always under-predicted vertical expansion, likely due to progressive leakage of the detonation products through the soil cap, which could not be entirely eliminated.

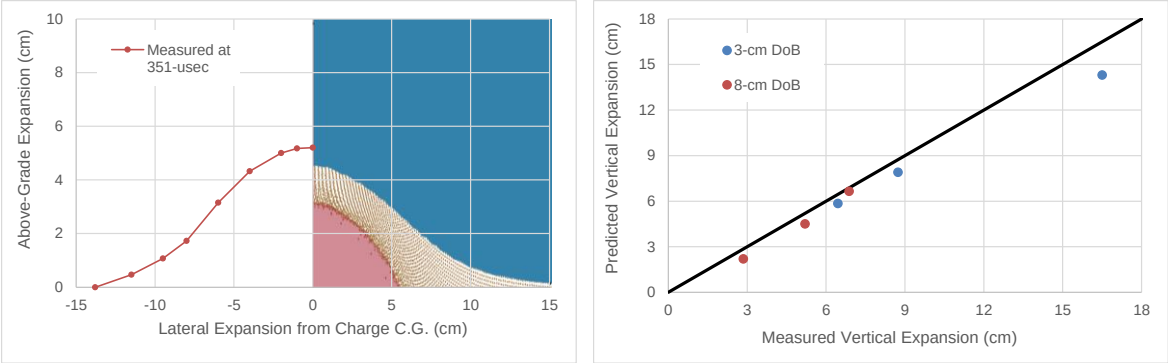

Figure 5. 8-cm DOB Soil Expansion Simulation for Hybrid SPH-ALE Modeling Strategy; Measurements Adapted from (17)

Models of Target Impact

LS-DYNA was used to simulate two series of landmine plate impact tests, which were conducted by the Ernst Mach Institute (EMI), per Anderson (6), and the Army Research Laboratory (ARL), Aberdeen Proving Ground (APG), per Skaggs (14)**.** These test series offered a range of charge sizes, plate shapes, and soil saturation conditions, of which a subset was chosen to evaluate the various LS-DYNA modeling strategies and the PEC sandy soil material modeling approach. In each case, imparted momentum and velocity histories were recorded for the target plate during each simulation for comparison with reported values.

ALE Models for Partially Saturated EMI Tests

The ALE modeling strategy was investigated for the EMI flat plate, 90-deg bent plate, and 120-deg bent plate impact scenarios using a 3-dimensional, quarter-symmetry computational domain, which was deemed necessary to correctly capture the geometry of the V-shaped target plates. The ALE domain in the region of the sonotube and plate was modeled with 5-mm bricks (10 elements through soil cap), and it dilated to progressively larger elements outside this region. It extended well beyond the sonotube radius and the target height to allow soil expansion and explosive circulation. The plate-to-soil friction coefficient was assumed to be 0.2.[1]

Following the development of the three-spring soil model, the material properties were automatically calculated using two *a priori* values: the dry density of the EMI test soil and the water content of the specific test case. Reports by Anderson, et al, listed the soil conditions during testing using moisture content and gross density (6) (7). The as-received sand was reported at 1.37 g/cm^3 with a moisture content of 7%; water was added to obtain two additional moisture content levels of 14% and 22%. The dry density of the material was calculated as 1.28 g/cm^3. Using the dry density and moisture contents for each species, compaction and strength curves were generated for each material, which were used for the EMI models of test series 1, 3, 4, 5, and 6. An example soil expansion renderings for the EMI 120-deg plate is shown in Figure 7.

[1] Per NAVFAC standards, as cited at http://www.finesoftware.eu/help/geo5/en/table-of-ultimate-friction-factors-for-dissimilar-materials-01/

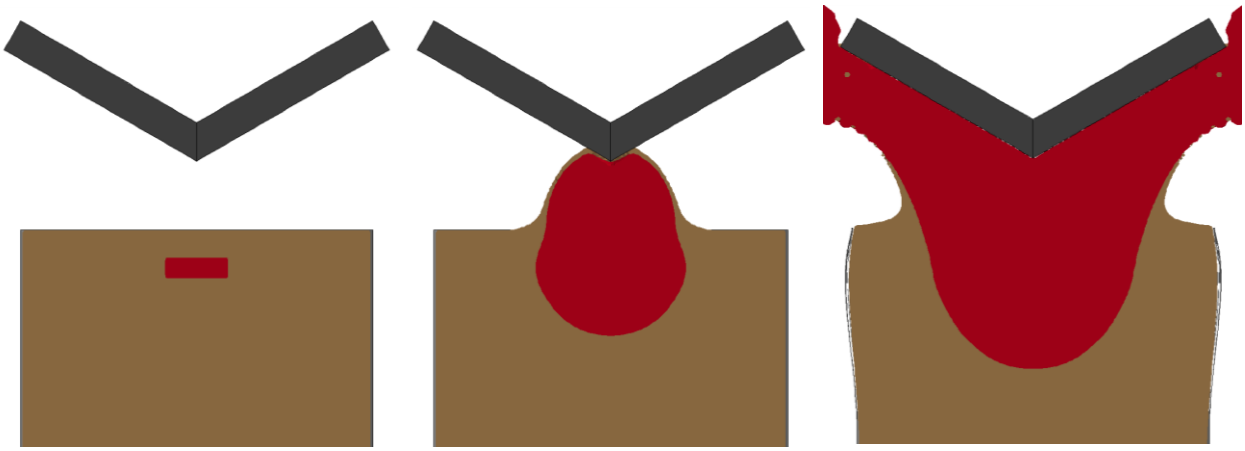

Figure 6. ALE Response Evolution for EMI 120-deg Bent Plate Impact Simulation

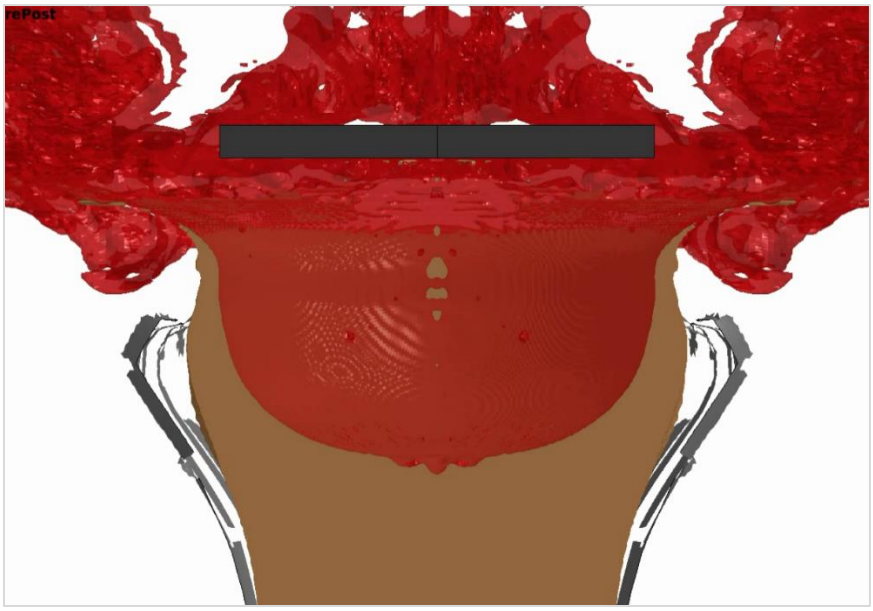

Figure 7. ALE Response Evolution for EMI Flat Plate Impact Simulation

Model results for five EMI cases are summarized and compared with predictions from prior researchers in Figure 9. The grey bars represent the average EMI experimental impulses, and the corresponding error bars show the experimental spread. The blue bars give the results obtained with PEC soil model, while the green bars show the predictions made with CTH by SwRI and with LS-DYNA by Schwer (7) (6) (15).

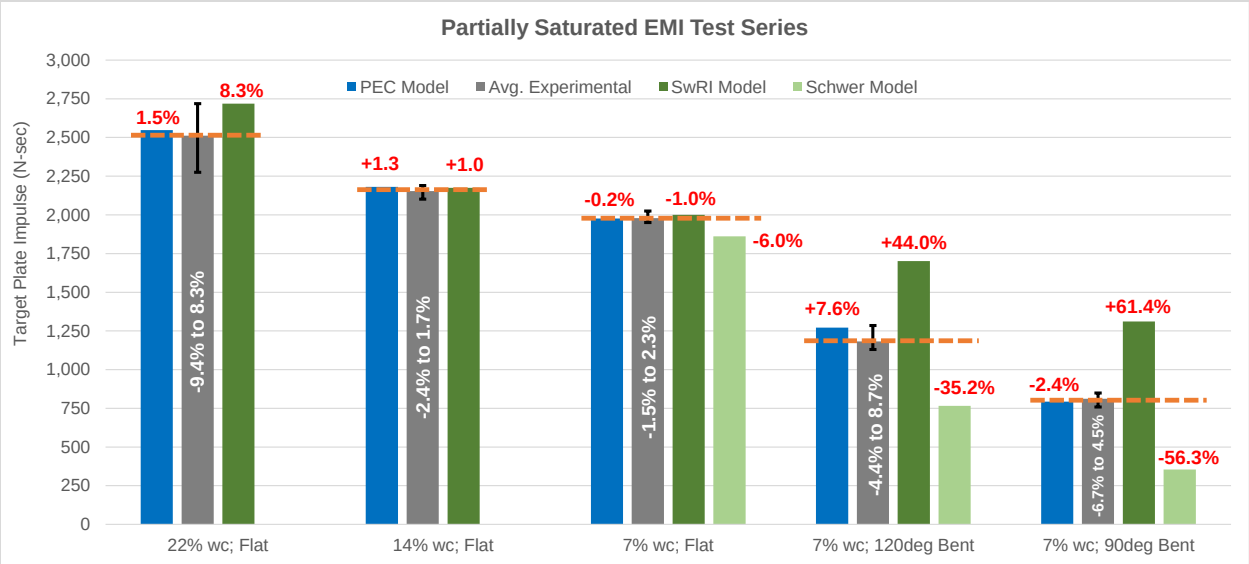

Figure 8. Comparison of EMI Experimental Impulses with Models by PEC, SwRI, and Schwer

A comparison of the trends reveals that the modeling of prior efforts tended to predict loading well for flat plate scenarios, but they diverge from experiment when V-shaped targets were introduced. CTH predictions from SwRI tended to over-predict impulse for the V-plates, while LS-DYNA simulations by Schwer tended to under-predict. In general, flat plate impulses seem to be easier to match, while the V-plates present a harder challenge and are more sensitive to material model and/or code differences.

The PEC model in LS-DYNA matched the loads for the bent plates well, falling within the error bars of the experimental tests in all cases. It should be noted that the average error for the V-plate cases in the prior modeling efforts was +/-50%, but the PEC model averaged about 5%: an order of magnitude reduction. The average error across all cases, including both flat and V-shaped targets, was under 3%. Irrespective of geometry, the PEC soil model appears to accurately replicate the EMI tests without *post hoc* material tuning.

A comparison of the impulses for the three test cases with 7% water content is shown in Figure 9, where the horizontal lines show the EMI experimental averages and bounds. Trends for the other test cases showed similar correspondence.

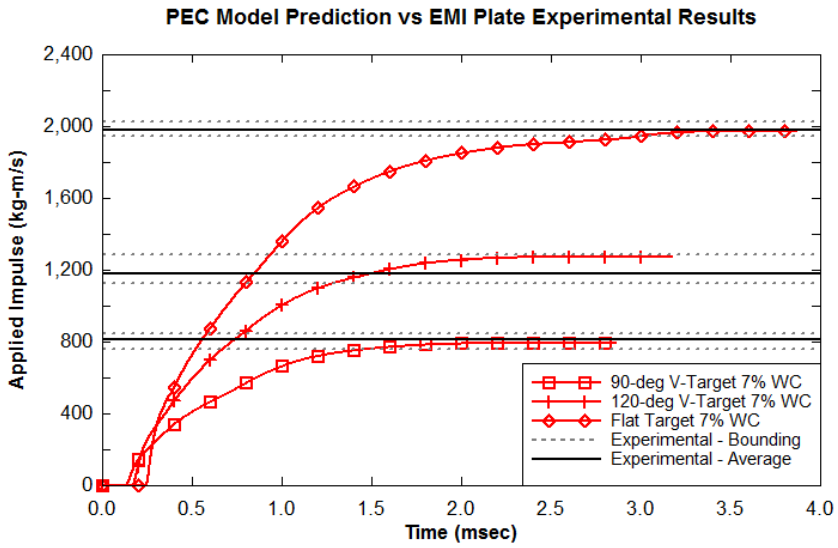

Figure 9. ALE Imparted Momentum for EMI Tests with 7% Water Content, PEC Soil Model

ALE Models for Fully Saturated VIMF Tests

The ALE models for the VIMF tests used an axisymmetric domain, because only a flat plate target was used and the soil domain was large. The target plate radius was modeled such that the axisymmetric plate would have the same surface area as the rectangular VIMF target. The ALE domain in the saturated test region (within the pool liner) was modeled with 5-mm bricks. It dilated to progressively larger elements outside this region.

Two cases from the experiment matrix were modeled. Both tests featured a 4.54-kg (10-lb) charge in fully saturated sand. The burial depth for the two tests was 0.1-m (4-in) and 0.3-m (12-in), while the plate standoff was 0.4-m (16-in). As with the EMI models, properties for the PEC three-spring compaction soil model were set *a priori* using two values: the dry density of the VIMF test soil and the fully-saturated water content. The dry density was 1.49 g/cm^3 and the fully saturated density at 1.91 g/cm^3 (16).

Grujicic modeled the VIMF tests using the CU-ARL constitutive model and published a comparison of the resulting predictions and the experimental impulses (14) (16). In comparing the test report and the paper, we noted apparent discrepancies between the reported experimental impulses, on the order of 30% to 60%. As such, the comparison between predictions and experiments was deemed uncertain (16). To avoid any potential ambiguity, we assumed the experimental impulses per the ARL report were correct and used them in our comparisons (14). Since the actual experimental values in the limited distribution ARL report have not, to our knowledge, been published in the open literature, they have been omitted from this paper and the impulse comparisons are relative.

The PEC soil model matched the loads for both tests well, with an average error of just under 2%. In contrast with the EMI test series, it should be noted that the charge size and impulse loads were an order of magnitude larger, and the soil was fully saturated, thus illustrating the versatility of the PEC approach across a range of saturation conditions and load severity.

SPH Models for Partially Saturated EMI Tests

The SPH models for the EMI tests used a quarter-symmetric 3-dimensional domain. SPH particles were used in a limited region of the domain due to computational costs. This region was immediately surrounding the charge, with a radius of 190-mm and a depth of 290-mm, using 2.5-mm particles. The SPH domain was coupled to an FEM brick domain outside this area, which made up the balance of the Sonotube volume. Models were run with both the default and renormalized particle formulations, but typically the default was used.

Trials of the SPH approach showed an instability related to the inclusion of air particles. The drastic difference in mass density between air and soil/high-explosive required the use of a particle-to-particle contact at the air-soil interface (*DEFINE_SPH_TO_SPH_COUPLING). In some cases this coupling worked well (Figure 10). As the SPH air particles become unstable, they shoot off at excessively high velocities through the computational domain, causing additional instabilities as the rogue particles collide with stable neighboring particles (Figure 11). In simulations that ran long enough before the onset of shooting particles, the air contribution was found to be small and to take place relatively early in time. Over longer simulation times with ALE, it was estimated that air contributed less than 3% of the total momentum. In light of the minor contribution and the intractable stability issues, air was neglected in the SPH plate impact models.

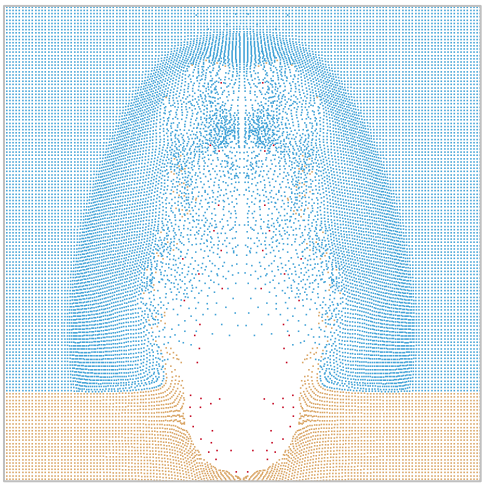

Figure 10. Stable SPH Air to Soil Particle Contact

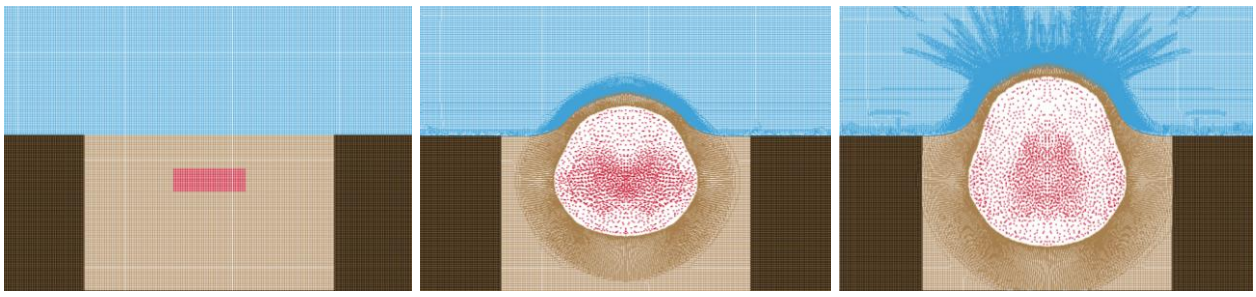

Figure 11. Unstable SPH Air to Soil Particle Contact Caused by Shooting Rogue Particles

Unlike the ALE formulation, the SPH formulation was found to generally under-predict peak imparted momentum; errors were approximately 15-percent or less for all target plate

configurations. From a standpoint of computational expense, the SPH simulations were markedly more costly than the ALE simulations.

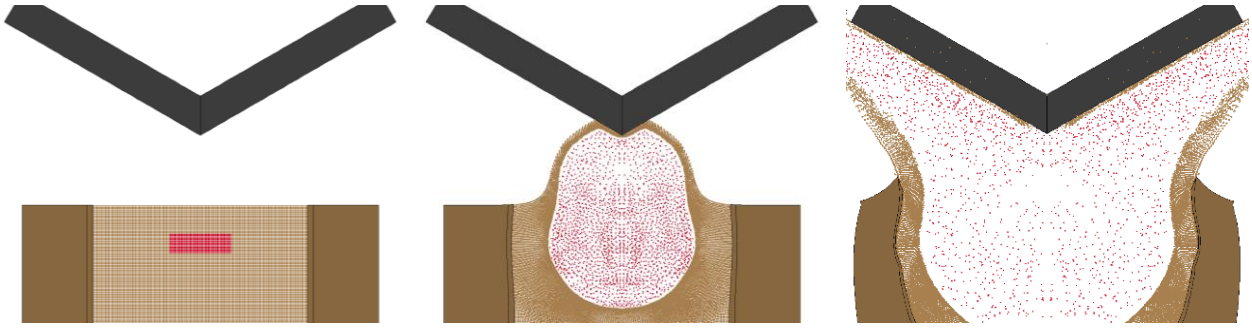

Figure 12. SPH Response Evolution for 120-deg Bent Plate Impact Simulation, Primitive Soil Model

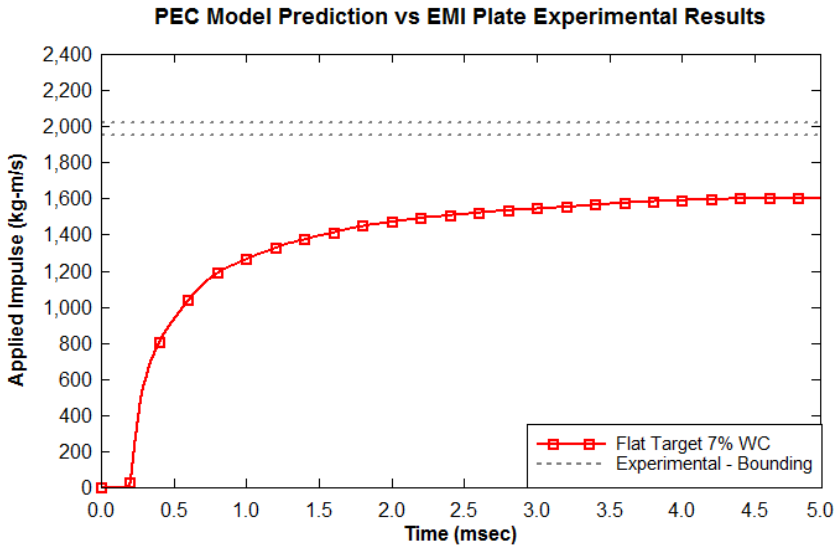

Figure 13. SPH Imparted Momentum for EMI Flat Plate Test with 7% Water Content, PEC Soil Model

Hybrid ALE-SPH Models of EMI Tests

Preliminary ALE-SPH hybrid models were constructed for the flat plate and 90-deg bent plate EMI tests. The ALE domain used 5-mm elements that contained air, explosive, and soil materials. It extended from 70-mm above the plate to 400-mm below the soil surface. The soil was represented with SPH particles in the vicinity of the buried charge, and the typical particle spacing was 2.5-mm (i.e., 8-to-1 ratio of SPH particles to a single ALE element). The soil transitioned to a FEM brick representation at a depth of 200-mm from the soil surface.

Numerical instabilities plagued the hybrid simulations, resulting in premature terminations that were unresolvable. A unique challenge associated with the hybrid ALE-SPH approach involved the FSI coupling algorithms required for the ALE-to-SPH interaction (*ALE_COUPLING_NODAL_PENALTY). Comparison of the incomplete impulse histories (not shown) with the pure SPH models showed worse under-prediction. Owing to the complexity, computational expense, and poor results, development of the hybrid approach was eventually suspended.

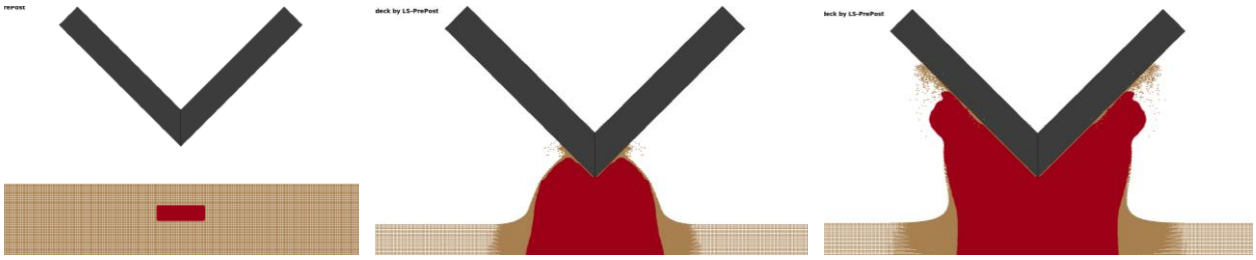

Figure 14. Hybrid SPH-ALE Response Evolution for 90-deg Bent Plate Impact Simulation (ALE air not shown)

Influence of ALE Mesh Discretization

The effects of ALE mesh size were examined to ensure that discretization error was not adversely influencing the results obtained. Since the EMI tests used smaller charge sizes and shallower burial depths than the VIMF tests, the flat plate 7% water content case was selected for evaluation. A set of simplified 2D axisymmetric ALE models were constructed with the same cross-sectional dimensions as the 3D models previously discussed. Mesh sizes of 10-mm, 6-mm, 5-mm, and 4-mm were evaluated. To eliminate confounding factors arising from fluid-structure coupling, the target plate was not explicitly modeled. Instead, constrained ALE nodes in the plate region provided a rigid virtual plate for load collection. The axisymmetric target radius was set to give a circular area equivalent to the rectangular test plate. Because the virtual target was fixed in space and massless, factors like inertial acceleration, gravity force, and resistance from air above the target were not included. As such, the load histories measured in these models are comparable to one another for evaluating discretization effects, but they not strictly comparable to the prior 3D inertial plate models.

Early loading and the time of arrival showed some mesh dependence, but the total impulse after 10 msec was not greatly affected by mesh size (Figure 15). The trend for total impulse proved to be fairly flat, with no clear convergence or divergence. It showed only a slight oscillation around the average value. The impulse range fell within +/-0.75% of the mean. This brief examination indicated that the use of 5-mm ALE meshes in the 3D models was appropriate, and that the mesh discretization errors were not unduly affecting the model results.

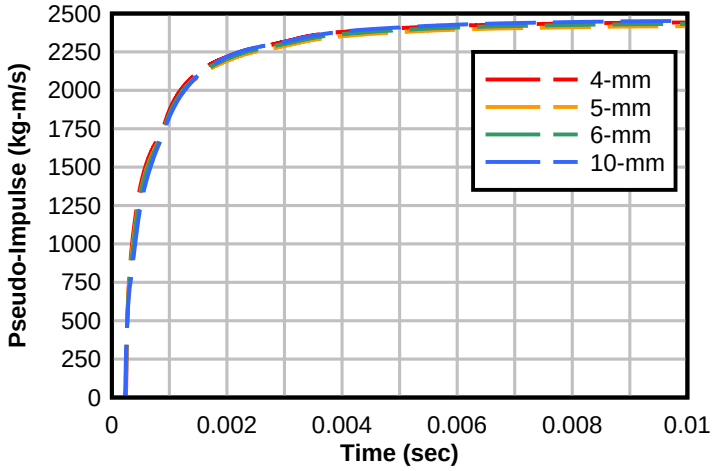

Figure 15. Impulse Histories for Different ALE Element Sizes, EMI Flat Plate 7% wc

Observations Regarding Material Properties and Accuracy

During the evaluations of the various modeling strategies and the development of the PEC sandy soil material modeling approach, several observations were made regarding the relationship of soil material properties and prediction accuracy. It was noted that density has a strong effect on impulse, while soil strength and plate friction proved to be much milder. Plate friction was largely negligible for flat plate impacts, but it proved to be non-negligible for the V-plate EMI tests, where sliding friction has a vertical component.

The most important observation made was with regard to the criticality of compression properties of the material, as defined in *EOS_TABULATED_COMPACTION. The effects of the compression curve were, if anything, more important than those of material density. Phenomenologically, the rapidly expanding explosive products are contained, at least in a transient sense, by the spongy soil surrounding them. The degree of compliance in this pseudo container determines how much energy is immediately absorbed from the expanding explosive products. Where the soil is fully saturated, and therefore proves less spongy and more confining, the sides and bottom of this soil container allow far less volume expansion, thereby driving the explosion energy upward with stronger directional bias. It was found that even slight errors in the compression curve, such as defining the strain at water lockup in partially saturated soils, led to substantial deviations in imparted momentum.

Simplifying assumptions regarding the compression curve may, in the author's view, be partly responsible for predictive inaccuracies in some of the prior modeling efforts surveyed in the literature. Adverse assumptions may include errors in estimating dry density, errors in defining the point of water lockup, linear assumptions regarding water compression, or failures to carry the compression curve to sufficiently high strains and related compression modulus.

Qualitatively, the experiences of this effort would suggest the following rank ordering for material properties as they relate to predicted impulse accuracy:

1. Compression curve
2. Density
3. Yield strength curve
4. Plate friction

Conclusions

Several LS-DYNA modeling strategies were evaluated for simulating landmine explosions, including ALE, SPH, hybrid ALE-SPH, eroding FEM to SPH, and DEM. Evaluations included the examination of initial soil bubble expansion and the imparted impulse on flat and V-shaped plate targets. The all-ALE formulation clearly produced the most accurate predictions of soil bubble expansion and target impulse; this proved true in all cases examined. While the all-SPH strategy was viable, it was computationally expensive and tended to under-predict impulse. Comparable accuracy to ALE may be possible, but likely only with even finer meshing and greater computational cost. The hybrid ALE-SPH strategy proved to be the most complicated

and least accurate approach for landmine modeling. Attempts with an eroding FEM to SPH strategy proved unstable and unreliable. The DEM approach was examined but not heavily investigated due to its inability, at least at the time of this research, to allow a priori constitutive property definition from soil material properties.

A notable accomplishment of this effort was the development of a generalized sandy soil model using a three-spring approach for defining the material compaction curve. The approach developed by PEC develops a full material model definition based on only two *a priori* input values: dry density and saturation percentage. The use of the PEC sandy soil model showed high accuracy across the full range of soil saturation, against a range of target shapes, and for widely varying charge sizes. No *post hoc* material tuning was employed to improve the correlation to experimental results. The average error was under 3%, with V-plates showing around 5% error, all of which was within the experimental data scatter. Accuracy was found to depend heavily upon the nuances of the compression curve and the density of the soil, while properties of material strength and plate friction proved to be of secondary importance.

References

1. *ARL-RP-98: Simulating the Blast of Buried Mines on Lightweight Vehicle Hulls.* **Cheeseman, Bryan A., et al., et al.** Monterey, CA : Army Research Laboratory, 2005. 15th Annual Ground Vehicle Survivability Symposium. ARL-RP-98.

2. **Moral, Ramon J., Danielson, Kent T. and Ehrgott, John Q. Jr.** *ERDC/GSL TR-10-27: Tactical Wheeled Vehicle Survivability: Comparison of Explosive-Soil-Air-Structure Simulations to Experiements Using the Impulse Measurement Device.* Geotechnical and Structures Laboratory, Engineer Research and Development Center. Vicksburg, MS : US Army Corps of Engineers, 2010. ERDC/GSL TR-10-27.

3. *Discrete Particle Approach to Simulate the Combined Effect of Blast and Sand Impact Loading of Steel Plates.* **Borvik, T., et al., et al.** 59, s.l. : Elsevier Ltd., March 2, 2011, Journal of the Mechanics and Physics of Solids, pp. 940-958.

4. **Danielson, Kent T., et al., et al.** *Lagrandian Meshfree Methodologies for Predicting Loadings from Buried Munitions Detonations.* U.S. Army Engineer Research and Development Center. Vicksburg, MS : s.n.

5. *The Effect of Degree of Saturation of Sand on Detonation Phenomena Associated with Shallow-Buried and Ground-Laid Mines.* **Grujicic, M., Pandurangan, B. and Cheeseman, B.A.** 12, s.l. : IOS Press, 2005, Shock and Vibration, pp. 1-21.

6. **Anderson, Charles E., et al., et al.** *18.12544/011: Mine-Blast Loading: Experiments and Simulations.* Southwest Research Institute. Herndon : US Army Tank-Automotive Research, Development and Engineering Center, 2010. 18.12544/011.

7. *Mine Blast Loading: Experiments and Simulation.* **Anderson, Charles E, et al., et al.** Herdnon, VA : ARL Research in Ballistic PRotection Technologies Workshop, 2010.

8. **Kerley, G I.** *The Effects of Soil Type on Numerical Simulations of Buried Mine Explosions: Report KTS02-3.* Appomattox, VA : Kerley Technical Services, 2002.

9. **Kerley, Gerald I.** *Documentation of Data on Sandia ANEOS Library File.* Albuquerque : Sandia National Laboratories, 2001.

10. **Bergeron, D, Walker, R and Coffey, C.** *Report 668: Detonation of 100-gram Anti-Personnel Mine Surrogate Charges in Sand: a Test Case for Computer Code Validation.* Alberta : Defense Research Establishment, Suffield, 1998.

11. *Derivation of Mechanical Properties for Sand.* **Laine, Leo and Sandvik, Andreas.** Singapore : CI-Premier PTE LTD, 2001. 4th Asia-Pacific Conference on Shock and Impact Loads on Structures. pp. 361-368.

12. **Kerley, G.I.** *ARL-CR-461: Numerical Modeling of Buried Mine Explosions.* s.l. : Aberdeen Proving Ground, 2001.

13. **Blouin, S E and Kwang, J K.** *Undrained Compressibility of Saturated Soil: Report DNA-TR-87-42.* Washington, DC : Defense Nuclear Agency, 1984. DNA-TR-87-42.

14. **Skaggs, R. Reed, Gault, William and Taylor, Leslie C.** *ARL-TN-250: Vertical Impulse Measurements of Mines Buried in Saturated Sand.* Weapons and Materials Research Directorate. Aberdeen Proving Ground, MD : U.S. Army Research Laboratory, 2006. ARL-TN-250.

15. **Schwer, Len.** *Simulations of SwRI Buried Charge Experiments.* Schwer Engineering & Consulting Services, SwRI. Windsor, CA : s.n., 2012.

16. *Impulse Loading Resulting From Shallow Buried Explosives in Water-Saturated Sand.* **Grujicic, M., et al., et al.** s.l. : Proc. IMechE, 2007, J. Materials: Design and Applications, Vol. 221, pp. 21-35.

17. *A Computational Analysis of Detonation of Buried Mines.* **Grujicic, M., Pandurangan, B. and Cheeseman, B.A.** s.l. : Brill, September 20, 2005, Multidiscipline Modeling in Mat. and Str., pp. 1-26.

18. **Veyera, George E.** *WL-TR-93-3523: Uniaxial Stress-Strain Behavior of Unsaturated Soils at High Strain Rates.* Wright Laboratory Flight Dynamics Directorate, Air Force Material Command. 1994. WL-TR-93-3523.

19. **Barsotti, Matt, Sammarco, Eric and Stevens, David J.** *Mitigation of Blast Injuries Through Modeling and Simulation: Task 1 Report: Soil and Explosive Modeling.* Quantico : United States Marine Corps MARCORSYSCOM, via Protection Engineering Consultants, 2015.